

ATLAS MUON TRIGGER PERFORMANCE

A. Policicchio¹ on behalf of the ATLAS Collaboration

¹ *Sapienza Università di Roma and INFN Roma1, Roma, Italy*

E-mail: antonio.policicchio@roma1.infn.it

Events containing muons in the final state are an important signature for many analyses being carried out at the Large Hadron Collider (LHC), including both standard model measurements and searches for new physics. To be able to study such events, it is required to have an efficient and well-understood muon trigger. The ATLAS muon trigger consists of a hardware based system, as well as a software based reconstruction. Due to the high luminosity in Run 2, several improvements have been implemented to keep the trigger rate low, while still maintaining a high efficiency. Some examples of recent improvements include requiring coincidence of hits in the muon spectrometer and the calorimeter and optimised muon isolation. An overview of the muon trigger, the recent improvements, and the performance in Run 2 data are presented. The improvements planned for Run 3 are also discussed.

Keywords: ATLAS, LHC, Muon, Trigger, TDAQ

Antonio Policicchio

Copyright © 2019 for this paper by its authors.

Use permitted under Creative Commons License Attribution 4.0 International (CC BY 4.0).

1. Introduction

Muons are a signature of many of the physics processes studied and searched for at the ATLAS experiment [1] at the Large Hadron Collider (LHC). The muon trigger system is thus an essential component of the experiment and it is designed to efficiently select events of interest for physics analyses. It consists of two components: the hardware-based Level-1 (L1) and the software-based high-level trigger (HLT). Events accepted at the fast L1 step are passed on to the HLT, which runs algorithms close to offline reconstruction to make a final trigger decision. The ATLAS muon trigger system has undergone continuous improvements in order to cope with the instantaneous luminosity and the large number of interactions per bunch crossing provided by the LHC during the Run 2. This allowed the muon trigger system to provide high quality muons over a large spectrum of transverse momentum (p_T) with high efficiency. In Run 3, the instantaneous luminosity of the LHC will be increased up to $3.0 \times 10^{34} \text{ cm}^{-2}\text{s}^{-1}$, 50% more with respect to the Run 2 highest luminosity. The L1 trigger rate exceeds the detector readout limitations when extrapolated to the luminosity expected during Run 3. Various upgrades of the muon trigger system will be deployed, in order to reduce the trigger rate while keeping the same performance as in Run 2. These proceedings present an overview of the muon trigger system and of the recent upgrades, as well as its performance measured in 2018 proton-proton collision data. The improvements planned for Run 3 are also discussed.

2. The ATLAS muon trigger

Muon triggers are based on the information provided by the muon spectrometer (MS) and the inner detector (ID). The MS consists of three large air-core superconducting toroidal magnets (two endcaps and one barrel) providing a field of approximately 0.5 T on average. The deflection of the muon trajectories in the bending plane of the magnetic field is measured via hits in three layers of monitored drift tube (MDT) precision chambers covering the region in pseudorapidity $|\eta| < 2.7$. In the innermost endcap wheels of the MS, cathode strip chambers (CSC) are used instead of MDTs in the region $2.0 < |\eta| < 2.7$. Three layers of resistive plate chambers (RPC) in the barrel ($|\eta| < 1.05$) and 3-4 layers of thin gap chambers (TGC) in the endcaps ($1.05 < |\eta| < 2.4$) allow for fast read-out to make the initial trigger decision at L1. The ID provides track measurements based on hits in the pixel, semiconductor tracker and transition radiation tracker, arranged in successive layers (with the pixel detector closest to the interaction point) surrounded by a solenoid providing a 2 T magnetic field. It covers a fiducial region up to $|\eta| = 2.5$. Higher resolution and precise tracking information provided by MDT and CSC chambers and ID are used to refine the trigger decision at the HLT. The locations of the detectors are shown in Figure 1 (left). The inner endcap disks made of the CSC and MDT chambers are also referred to as the Small Wheels (SW), the external disks as the Big Wheels (BW).

2.1. Level-1 muon trigger

The L1 trigger identifies muons using coincidence requirements on the hits provided by the RPCs or TGCs. To estimate the p_T of the muons, the deviation from the hit pattern of an infinite momentum assumption is used to define six L1 thresholds in the p_T range 4 - 20 GeV. The L1 trigger identifies Regions of Interest (RoIs) in the detector, and the information is passed to the HLT. In the barrel region, for the three high p_T thresholds, hits in all three layers are required, while for the remaining low p_T thresholds (up to 10 GeV) the hit requirement is loosened to two coincidence hits.

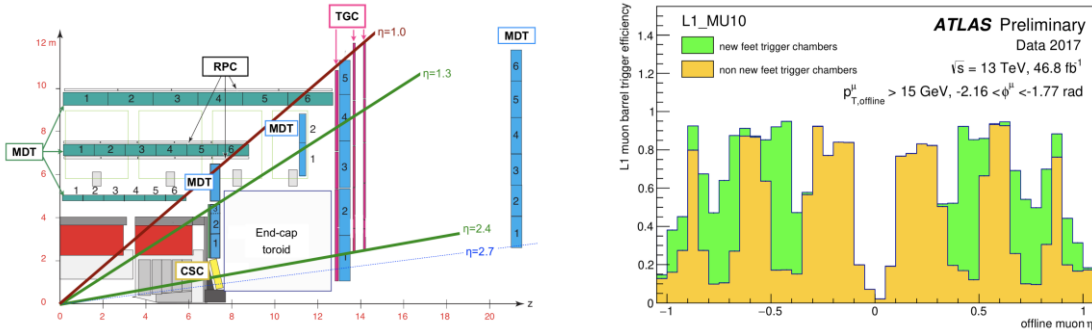


Figure 1. Left: schematic picture showing one quarter of a cross section of the ATLAS detector [2]. Right: Efficiency of L1 10 GeV muon trigger including (green) or excluding (yellow) the trigger chambers in the feet region of the detector. The efficiency is computed with respect to offline muon candidates and it is plotted as a function of the η for a specific sector $-2.16 < \phi < -1.77$ rad of the feet region [3]

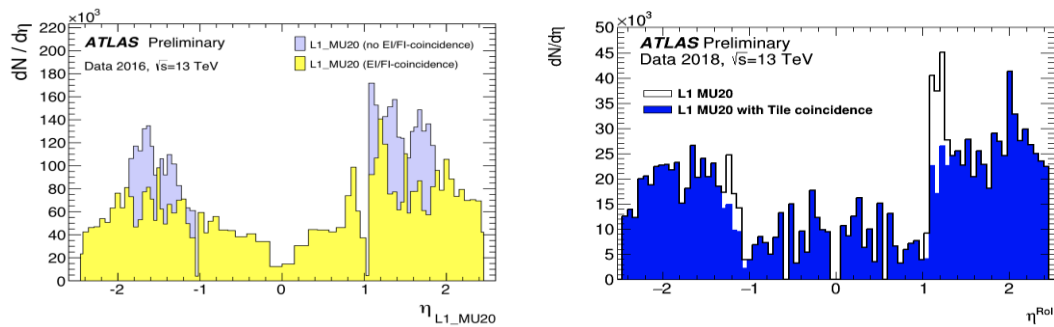


Figure 2. Left: The η distributions of the L1 20 GeV muon candidates (grey) and the rate reduction effect by the EI/FI coincidence (yellow) [4]. Right: Comparison between η of the L1 20 GeV muon candidates passing the EI/FI coincidence (white) and the subset which passes the hadronic tile calorimeter coincidence (blue) [3]

In the endcaps the coincidence in three layers is required for all thresholds. To increase the coverage, additional RPC chambers have been installed in 2015 in the regions of the feet that support the ATLAS detector. Figure 1 (right) shows the L1 muon trigger efficiency for the L1 muon trigger with 10 GeV p_T threshold in the feet region as a function of the pseudorapidity. The increase of efficiency due to the additional RPC chambers is shown by the green area. In the endcaps, to reduce fake muon contributions from particles not originating from the interaction point, an additional coincidence of the SW TGCs in the forward inner (FI) and endcap inner (EI) chambers has been introduced in 2016. As shown in Figure 2 (left) for the 20 GeV L1 muon trigger, fake muons are significantly suppressed ($\sim 20\%$). Further rate reduction has been achieved enabling a TGC coincidence with the extended barrel region of the hadronic tile calorimeter (TileCal). The resulting rate reduction ($\sim 6\%$) is shown in Figure 2 (right) for the 20 GeV L1 muon trigger.

2.2. High level muon trigger

The muon reconstruction at the HLT is split into fast and precise reconstruction steps. Starting from the L1 RoI, in the fast reconstruction step, the MDT hits are used to refine the muon candidate provided by the L1. First, muon candidates are built by performing a track fit based on the precision measurement of drift times and positions in the MDT chambers (MS-only track). The transverse momentum is assigned using look-up tables. The MS-only track is then extrapolated to the interaction point and combined with tracks reconstructed in the ID, forming combined muon candidates. In 2016

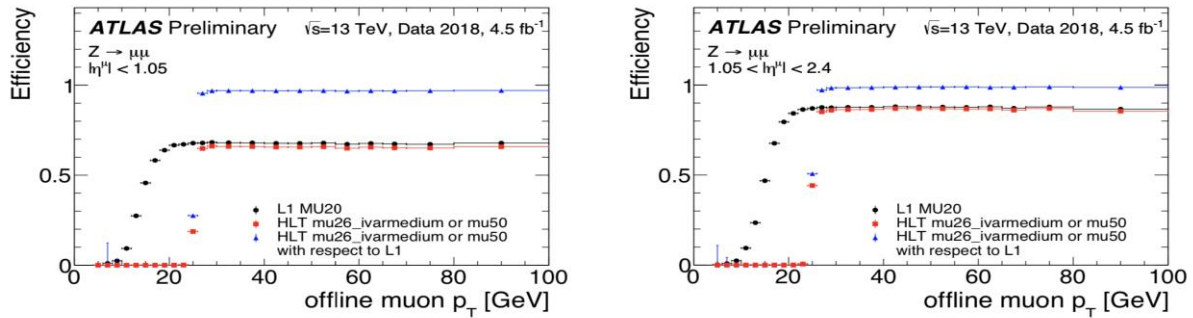


Figure 3. Absolute L1 (black), and absolute (red) and relative (blue) HLT muon trigger efficiencies measured in $Z \rightarrow \mu\mu$ events as a function of the offline muon p_T in the barrel (left) and endcap (right) regions [4]. At L1, a muon trigger with a p_T threshold of 20 GeV is shown, the events at the HLT step pass either a trigger with a 26 GeV p_T requirement and an isolation cut, or a trigger requiring $p_T > 50$ GeV

an additional measurement outside the magnetic field has been introduced to extrapolate to hits in the CSC layer and improve the p_T resolution in the highest pseudorapidity endcap region. If the fast reconstruction step is passed, the muon candidate enters the precision step. Track reconstruction exploiting the information from all MS detectors is performed. MS-only muon candidates are built first and are subsequently combined with precision ID tracks to form combined muons. In addition to the extrapolation from the MS to the ID (outside-in), there exists another algorithm that extrapolates ID tracks to the MS in case the former fails (inside-out). This recovers about 1-5% of muons depending on the muon p_T . To recover efficiency losses from the L1 trigger, another algorithm searches for muon candidates in the full detector. As this is very CPU expensive, it is used in di-muon triggers where one muon passed the baseline sequence and the second muon is searched for in the full detector. MS-only muon triggers are also available. In this case the muon reconstruction is only run in the MS. MS-only triggers are vital e.g. in searches for long-lived particles (displaced decays of long-lived particles may result in muons with no connecting tracks in the ID). To cope with the rate limitations, isolation criteria may be applied on the muon candidates built at the HLT. Isolation requires that there is little activity in the detector around the muon candidate by cutting on the relative p_T sum of ID tracks in a cone around the muon candidate with respect to the p_T of the muon candidate.

2.3. Efficiency measurement in 2018 pp collision data

Muon trigger efficiencies are measured exploiting $Z \rightarrow \mu\mu$ (J/ψ for low p_T triggers) events in a tag-and-probe method [5]. Figure 3 shows the L1 and HLT muon trigger efficiencies as a function of the offline reconstructed muon p_T using data collected in 2018 for barrel and endcaps. At L1, a muon trigger with a p_T threshold of 20 GeV is shown, the events at the HLT step pass either a trigger with a 26 GeV p_T requirement and an isolation cut, or a trigger requiring $p_T > 50$ GeV. The L1 trigger efficiency is limited by the coverage of trigger chambers, while the HLT with respect to L1 is almost 100% efficient. A sharp turn-on curve of the trigger efficiency at the HLT is visible above the trigger p_T threshold. The efficiencies in the endcaps are higher than in the barrel, mostly caused by detector geometric coverage ($\sim 80\%$ in barrel).

3. Outlook for LHC Run 3

In the ATLAS upgrade foreseen for the LHC Run 3, the SW will be replaced by the New Small Wheels (NSW). The NSW will consist of small-strip TGC and Micro-Mesh Gaseous Structure chambers that will be used for both triggering and precision tracking [6]. In the barrel-endcap transition region ($1.05 < |\eta| < 1.3$), the MDT chambers will be replaced by integrated stations of new

generation RPC and small-diameter MDT chambers to enhance the trigger coverage (BIS7/8 project [7]). The excellent online tracking capabilities of the new detectors will be used to improve the online muon identification in order to identify and reject fake muons and thus reduce the L1 trigger rate. A schematic diagram of the improved trigger algorithm for muon identification in the endcap region is shown in Figure 4 (left). In the current scheme, tracks A, B and C are identified as L1 muons by the BW station. In the new trigger scheme, tracks are identified as muons only if they have coincidence hits in both the NSW and BW stations. In addition, the candidate muon track segment reconstructed in the NSW must point to the interaction point. Fake muons (tracks B and C) typically do not have these features and would be rejected by the algorithm. For a L1 20 GeV muon trigger a rate reduction by a factor ~ 2 is estimated, allowing to keep the same Run 2 trigger thresholds with the same performance. Figure 4 (right) shows the pseudorapidity distribution of the L1 20 GeV muon candidates in 2017 data, the distributions when enabling hadronic tile calorimeter coincidence, and when enabling the RPC BIS7/8 and NSW coincidences.

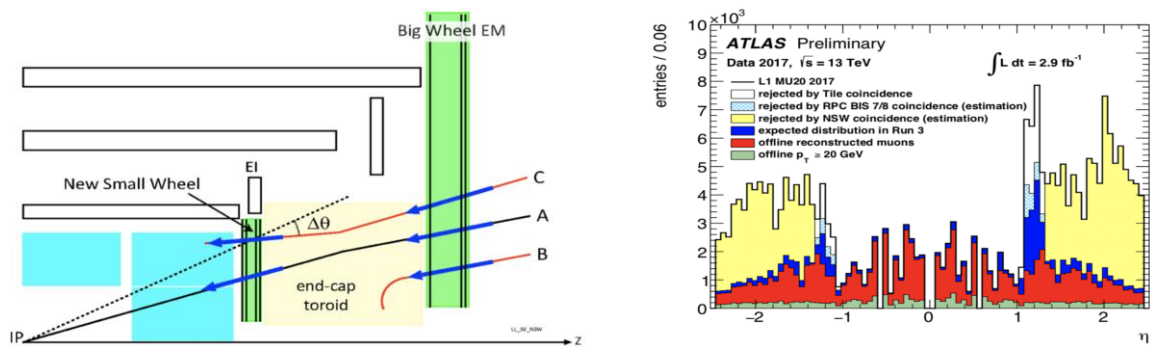


Figure 4. Left: Schematic diagram of the proposed Run 3 trigger algorithm used for fake muon discrimination viewed in one quarter of a cross section of the ATLAS detector [6]. Right: The η distribution of the L1 20 GeV muon candidates (black line); the L1 20 GeV muon candidates rejected when enabling the hadronic tile calorimeter (white), the RPC BIS7/8 (pale blue) and NSW (yellow) coincidences; the expected distribution of L1 20 GeV muon candidates in Run 3 after enabling all hadronic tile calorimeter, RPC BIS7/8, and NSW coincidences (blue); the distribution of all offline muon candidates (red) and of the offline muon candidates with $p_T > 20$ GeV [3]

References

- [1] ATLAS Collaboration, The ATLAS Experiment at the CERN Large Hadron Collider, JINST 3 S08003.
- [2] ATLAS Collaboration, ATLAS muon spectrometer: Technical Design Report, CERN-LHCC-97-022, <https://cds.cern.ch/record/331068>.
- [3] ATLAS Collaboration, L1 Muon Trigger Public Results, <https://twiki.cern.ch/twiki/bin/view/AtlasPublic/L1MuonTriggerPublicResults>.
- [4] ATLAS Collaboration, Public muon trigger results, <https://twiki.cern.ch/twiki/bin/view/AtlasPublic/MuonTriggerPublicResults>.
- [5] ATLAS Collaboration, Muon reconstruction performance of the ATLAS detector in proton-proton collision data at $\sqrt{s} = 13$ TeV, Eur. Phys. J. C (2016) 76:292.
- [6] ATLAS Collaboration, New Small Wheel Technical Design Report, CERN-LHCC-2013-006, <https://cds.cern.ch/record/1552862>.
- [7] ATLAS Collaboration, Technical Design Report for the Phase-II Upgrade of the ATLAS Muon Spectrometer, CERN-LHCC-2017-017, <https://cds.cern.ch/record/2285580>.